

Acknowledgments

One of the authors (I. G. Bromilow) was supported by a Science and Engineering Research Council CASE award in conjunction with Rolls-Royce Ltd., Bristol, U.K. The help from both organizations is gratefully acknowledged.

References

¹Zarodny, S. J. and Greenberg, M. D., "On a Vortex Sheet Approach to the Numerical Calculation of Water Waves," *Journal of Computational Physics*, Vol. 11, March 1973, pp. 440-446.
²Zalosh, R. C., "Discretized Simulation of Vortex Sheet Evolution with Buoyancy and Surface Tension Effects," *AIAA Journal*, Vol. 14, Nov. 1976, pp. 1517-1523.
³Daly, B. J., "A Technique for Including Surface Tension Effects in Hydrodynamic Calculations," *Journal of Computational Physics*, Vol. 4, 1969, pp. 97-117.
⁴Baker, G. R., Meiron, D. I., and Orszag, S. A., "Vortex Simulations of the Rayleigh-Taylor Instability," *Physics of Fluids*, Vol. 23, Aug. 1980, pp. 1485-1490.
⁵Clements, R. R. and Maull, D. J., "The Representation of Sheets of Vorticity by Discrete Vortices," *Progress in Aerospace Sciences*, Vol. 16, 1975, pp. 129-146.
⁶Bromilow, I. G. and Clements, R. R., "Some Techniques for Extending the Application of the Discrete Vortex Method of Flow Simulation," *Aeronautical Quarterly*, Vol. 33, May 1982, pp. 73-89.
⁷Rosenhead, L., "The Formation of Vortices from a Surface of Discontinuity," *Proceedings of the Royal Society, Ser. A*, Vol. 134, 1931, pp. 170-192.
⁸Hama, F. R. and Burke, E. R., "On the Rolling up of a Vortex Sheet," University of Maryland Technical Note BN-220, 1960.
⁹Chandrasekhar, S., *Hydrodynamic and Hydromagnetic Stability*, Oxford University Press, 1961, pp. 428-435.
¹⁰Drazin, P. G., "Kelvin-Helmholtz Instability of Finite Amplitude," *Journal of Fluid Mechanics*, Vol. 42, June 1970, pp. 321-335.

The Two-Dimensional Laminar Wake with Initial Asymmetry

Anthony Demetriades*

Montana State University, Bozeman, Montana

A FREQUENT problem in laser cavity flows, airfoil aerodynamics, and similar two-dimensional fluid problems is the mixing of two identical uniform, compressible streams past a sharp trailing edge (TE) of a partition, on one side of which the laminar boundary layer is thicker than it is on the other. Since the streams are identical, this configuration resembles an ordinary two-dimensional wake; however, the disparity in the boundary-layer thicknesses is bound to introduce asymmetries in the flow, especially beyond but near the trailing edge. The distance beyond the latter over which such asymmetries persist is of significance, especially if no restrictions are placed on the flow Mach number M_e and the temperature ratio T_w/T_{oe} of the solid partition relative to the stagnation temperature of the stream. This Note aims at presenting formulas valid for such an asymmetric wake for any M_e and T_w/T_{oe} and any degree of asymmetry introduced via the ratio $P = \theta_1/\theta_2$, where θ is the boundary-layer momentum thickness at the trailing edge and subscripts 1 and 2 refer to the two sides of the partition.

Received Feb. 12, 1982; revision received Dec. 20, 1982. Copyright © American Institute of Aeronautics and Astronautics, Inc., 1983. All rights reserved.

*Professor, Department of Mechanical Engineering. Associate Fellow AIAA.

For initially asymmetric wakes (arbitrary $0 < P < \infty$) the method used here is based on the linearized analysis of Gold¹ for wakes with arbitrary initial profiles. Gold's analysis used the Oseen linearization and a Chapman-Rubensin factor of unity. The Prandtl number, left arbitrary by Gold, was here assumed to be unity, to be consistent with the use of the Crocco relation connecting the fluid, wall (or TE), and stream (or wake "edge") temperatures T , T_w , and T_e , respectively,

$$\frac{T}{T_e} = \frac{T_w}{T_e} + \left(1 + \frac{\gamma-1}{2} M_e^2 - \frac{T_w}{T_e}\right) \frac{u}{u_e} - \frac{\gamma-1}{2} M_e^2 \left(\frac{u}{u_e}\right)^2 \quad (1)$$

where u is the flow velocity and $()_e$ denotes the edge conditions. The specific heat ratio γ was taken to be 1.4 in the computations shown below and the pressure was assumed to be everywhere constant.

The present calculation will be shown here in summary, since its details can be found in Ref. 2. The stretched longitudinal and lateral distances are given in terms of the physical coordinates x^* and y^* and the Reynolds number

$$Re_{\theta} \equiv \frac{u_e(\theta_1 + \theta_2)}{\nu_e} = \frac{u_e}{\nu_e} \Theta, \quad (\Theta \equiv \theta_1 + \theta_2) \quad (2)$$

by

$$x \equiv \frac{x^*}{\Theta Re_{\theta}}, \quad y \equiv \frac{1}{\Theta} \int_0^{y^*} \frac{\rho^*}{\rho_e^*} dy^* \equiv \frac{\bar{y}}{\Theta} \quad (3)$$

where ρ^* is the density. If the velocity profiles assumed at the TE ($x = x^* = 0$) are of the type

$$y^*, y > 0: \quad 1 - \frac{u}{u_e} = e^{-\bar{y}/\theta_1} = e^{-\frac{P+1}{P}y} \quad (4)$$

$$y^*, y < 0: \quad 1 - \frac{u}{u_e} = e^{\bar{y}/\theta_2} = e^{(P+1)y} \quad (5)$$

then one can obtain

$$\begin{aligned} \bar{u} &\equiv 1 - \frac{u}{u_e} = \bar{u}(x, y; M_e, T_w/T_{oe}, P) \\ &= \frac{1}{2} \left\{ \exp(P+1)^2 x + (P+1)y \right. \\ &\quad \times \left[1 - \text{Erf} \left((P+1)\sqrt{x} + \frac{y}{2\sqrt{x}} \right) \right] \\ &\quad + \left(\exp \left[\left(\frac{P+1}{P} \right)^2 x - \left(\frac{P+1}{P} \right) y \right] \right) \\ &\quad \times \left. \left[1 + \text{Erf} \left(\frac{y}{2\sqrt{x}} - \frac{P+1}{P} \sqrt{x} \right) \right] \right\} \quad (6) \end{aligned}$$

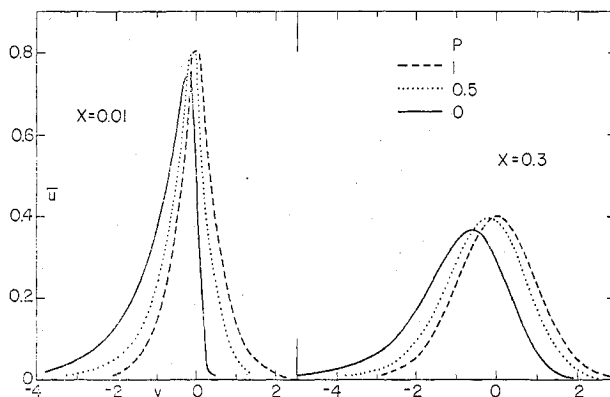


Fig. 1 Wake profiles as a function of $P = \theta_1/\theta_2$ and distance x from the trailing edge.

and

$$\begin{aligned} \bar{h} &\equiv \frac{T}{T_e} - 1 = \bar{h}(x, y; M_e, T_w/T_{oe}, P) \\ &= \frac{1}{2} \left\{ B \left[\exp \left[\left(\frac{P+1}{P} \right)^2 x - \frac{P+1}{P} y \right] \right. \right. \\ &\quad \times \left[1 - \operatorname{Erf} \left(\frac{P+1}{P} \sqrt{x} - \frac{y}{2\sqrt{x}} \right) \right] + \exp \{ (P+1)^2 x + (P+1)y \} \\ &\quad \times \left. \left. \left[1 - \operatorname{Erf} \left[(P+1)\sqrt{x} + \frac{y}{2\sqrt{x}} \right] \right] \right] \right\} \\ &\quad + C \left[\exp \left[4x \left(\frac{P+1}{P} \right)^2 - 2 \left(\frac{P+1}{P} \right) y \right] \right. \\ &\quad \times \left. \left. \left[1 - \operatorname{Erf} \left(2\sqrt{x} \frac{P+1}{P} - \frac{y}{2\sqrt{x}} \right) \right] \right. \right. \\ &\quad \left. \left. + \exp \{ 4(P+1)^2 x + 2(P+1)y \} \right. \right. \\ &\quad \left. \left. \times \left[1 - \operatorname{Erf} \left[2(P+1)\sqrt{x} + \frac{y}{2\sqrt{x}} \right] \right] \right] \right\} \\ B &= \frac{\gamma-1}{2} M_e^2 - 1 + \frac{T_w}{T_e} \\ C &= -\frac{\gamma-1}{2} M_e^2 \end{aligned} \quad (7)$$

It is easy to show from Eqs. (6) and (7) that the initial profiles [Eqs. (4) and (5)] are recovered for $x=0$, that $\bar{u}(x=\infty) = \bar{h}(x=\infty) = 0$ and $\bar{u}, \bar{h}(y=\pm\infty) = 0$, and that $\bar{u}, \bar{h}(y; P) = \bar{u}, \bar{h}(-y; 1/P)$, as expected. Furthermore, in the limit of large x the solutions reduce to the familiar asymptotic form for laminar wakes, which do not contain P and depend only on the similarity variable $y/2\sqrt{x}$.

Since experimental data with $P \neq 0$ are unavailable, a minimum validity check of these formulas should be their ability to reproduce, in the limit $P=1$, the classical two-dimensional wake solution found originally by Goldstein³ and subsequently verified independently by Au and Berger,⁴ Zeiberg and Kaplan,⁵ and others.⁶ Indeed, for the case of symmetry there is good mutual agreement among these theories, including the present one. For example, when $P=1$

Eq. (6) gives

$$\bar{u}(y=0) = \exp[4x(1 - \operatorname{Erf}2\sqrt{x})] \quad (8)$$

which agrees with Goldstein's result over $0 < x < \infty$ within a maximum difference of 2%. Within their scatter, the available experimental data for symmetric wakes also confirm the above theory, at both low⁷ and high^{2,4} speeds.

The effect of initial asymmetry, present when $0 < P < 1$, is evidenced by an asymmetry in the flow profiles and a displacement of the minimum-velocity point of the profile away from the $y=0$ plane. Computations made with Eqs. (6) and (7) indicate that both of these effects increase monotonically when P decreases from 1 toward 0. Figure 1 shows that the profile asymmetry begins to vanish by $x=0.3$ even in the extreme case of $P=0$. Beyond about $x=1$ the profiles become symmetrical regardless of P and coincide with the $P=1$ profile, except for a lateral displacement toward the side of the initially thicker boundary layer. This displacement corresponds to the position y where the minimum velocity is observed, and is illustrated on Fig. 2 again for $P=0, 0.5$, and 1. Note that the displacement is largest when P attains its extreme value of zero and is, of course, suppressed when P tends to unity. Figure 2 also shows the minimum profile velocity (the maximum in \bar{u}), which can be found at any distance x , and its dependence on P . It is seen that the minimum velocity does not depend greatly on P ; even for very small P it differs by only a few percent from the corresponding velocity for the symmetric wake. The general conclusions drawn from Figs. 1 and 2 are that initial asymmetry affects only the shape of the profile and that even this effect vanishes soon after $x=1$.

It should be stressed that the present approach is based on the Oseen approximation,¹ which assumes that the velocity variations across the wake are but a small fraction of the stream velocity. Like similar theories^{4,5} employing some type of linearization, the present method is also in good agreement with Goldstein's results near the trailing edge where these velocity variations are large.

A possible explanation for the observed agreement is that the present solution is constrained to obey the initial conditions at the TE ($x=0$) as well as the conditions at $y=\pm\infty$; the Oseen approach then also guarantees the proper behavior at large x . Apparently, these constraints dominate the solution to the point where the linearization restrictions assume a lesser role. As for the asymmetry feature of the present approach, a direct check must await the performance of numerical calculations or the publication of experimental results.

Acknowledgments

This work was supported jointly by TETRA Corporation and by the U.S. Air Force Office of Scientific Research under Contracts F44620-75-C-0016 and F49620-79-C-0210.

References

- Gold, H., "Laminar Wake with Arbitrary Initial Profiles," *AIAA Journal*, Vol. 2, May 1964, pp. 948-949.
- Demetriades, A., "The Compressible Laminar Two-Dimensional Wake with Arbitrary Initial Asymmetry," Mechanical Engineering Department, Montana State University, Bozeman, Rept. MSU/SWT 81-3, July 1981.
- Goldstein, S., "On the Two-Dimensional Steady Flow of a Viscous Fluid Behind a Solid Body—I, II," *Proceedings of the Royal Society of London, Series A*, Vol. 142, 1933, pp. 545-573.
- Au, H. C. and Berger, S. A., "A Theoretical and Experimental Investigation of the Compressible Wake Behind a Long Slender Cylinder," *AIAA Journal*, Vol. 6, Aug. 1968, pp. 1528-1534.
- Zeiberg, S. L. and Kaplan, B., "Approximate Analysis of Free Mixing Flows," *AIAA Journal*, Vol. 3, March 1965, pp. 552-554.
- Berger, S. A., *Laminar Wakes*, American Elsevier Publishing Co. Inc., New York, 1971, Chap. 2.

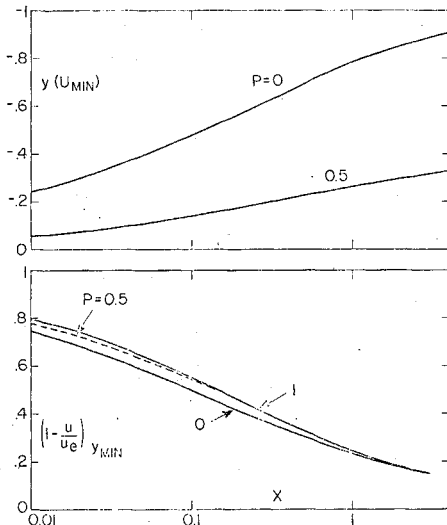


Fig. 2 Deflection distance (top) and magnitude (bottom) of the minimum velocity.

⁷Sato, H. and Kuriki, K., "The Mechanism of Transition in the Wake of a Thin Flat Plate Placed Parallel to a Uniform Flow," *Journal of Fluid Mechanics*, Vol. II, Pt. 3, Nov. 1961, pp. 321-352.

Boundary-Layer and Turbulence Intensity Measurements in a Shock Wave/Boundary-Layer Interaction

S. Raghunathan* and R. J. W. McAdam†
The Queen's University of Belfast, Northern Ireland

Nomenclature

- e_f^2 = root mean square voltage
- f = frequency
- H = compressible shape parameter, $= \delta^*/\theta$
- l_s = length of separated flow region
- M_{pk} = peak Mach number
- n = frequency parameter, $= fy/U_\infty$
- Tu_∞ = freestream turbulence intensity, $= \tilde{u}/U_\infty$
- Tu = turbulence intensity in boundary layer
- u = velocity
- \tilde{u} = root mean square velocity fluctuation
- U_∞ = freestream velocity
- U_{BS} = freestream velocity before shock
- y = vertical ordinate
- δ = boundary-layer thickness

Subscripts

- 1 = conditions before shock at station 1
- 2 = conditions at the trailing edge of the model

Introduction

PREVIOUS work by the authors has shown that attached turbulent boundary layers at zero pressure gradient are sensitive to the freestream turbulence.¹ The effect of freestream turbulence on the boundary layer at positive pressure gradients is very little understood.² An investigation of the influence of freestream turbulence on shock induced separation is presented in this Note.

Experiments

Experiments were performed in a 10-cm² transonic suction tunnel with a slotted floor.¹ The model was a roof-mounted half-biconvex aerofoil (9 deg thick). During the tests the peak Mach number was $M_{pk} = 1.44$ before the shock. This resulted in a flow separation at the foot of the shock followed by reattachment on the tunnel roof downstream of the trailing edge of the model (Fig. 1). Boundary-layer and hot-wire traverses were made at stations just upstream of the shock and in the separated region at the trailing edge. The freestream turbulence was varied by monoplane grids, the details of which are given in Ref. 1. The freestream turbulence was within the range 0.3-6.0%.

Results and Discussions

Velocity profiles upstream of the shock and downstream at the trailing edge of the model are shown in Fig. 1. The profiles

shown here are for a shock Mach number of 1.44 and freestream turbulence levels of $Tu_\infty = 0.34$ and 3.68%. The profiles are normalized with respect to the corresponding upstream boundary-layer thickness δ_1 . The boundary layer upstream of the shock is in a region of negative pressure gradient and has a "full" velocity profile. Increase in Tu_∞ results in a fuller velocity profile. The velocity profile at the trailing edge shows that the flow is completely separated. It appears that the separated layer becomes thinner with larger values of Tu_∞ . This is obviously due to increase in momentum exchange between the freestream and the separated layer at larger values of Tu_∞ . Thus, there is an influence of the freestream turbulence and the boundary layer in the entire region of the shock/boundary-layer interaction.

Figure 2 shows for various freestream turbulence levels the boundary-layer integral properties in the separated layer at the trailing edge expressed as a fraction of the corresponding properties upstream of the shock. It is observed that for $Tu_\infty < 2\%$, the displacement thickness ratio δ_2^*/δ_1^* and the shape factor ratio H_2/H_1 are very sensitive to Tu_∞ but the momentum thickness ratio θ_2/θ_1 is not sensitive to Tu_∞ . The values obtained here at low Tu_∞ are comparable to those measured by Kooi³ and Delery⁴ at identical Mach number and at similar locations. Kooi measurements were performed on a flat plate with a shock generator, whereas those of Delery were performed on an aerofoil. The freestream turbulence was not measured in both cases.

The longitudinal turbulence intensity distribution at the two locations and for $Tu_\infty = 0.34$ and 3.68% are shown in Fig. 3. The turbulence fluctuation levels are normalized with respect to the corresponding freestream velocities upstream of the shock. The turbulence intensity profiles show a strong interaction between the freestream turbulence and the boundary-layer turbulence in the outer region of the attached boundary layer and the separated layer. The peak levels of turbulence in the attached boundary layer near the shock are close to the measured peak values on an attached boundary layer at zero pressure gradient. However, the turbulence is likely to have become anti-isotropic upstream of the shock.

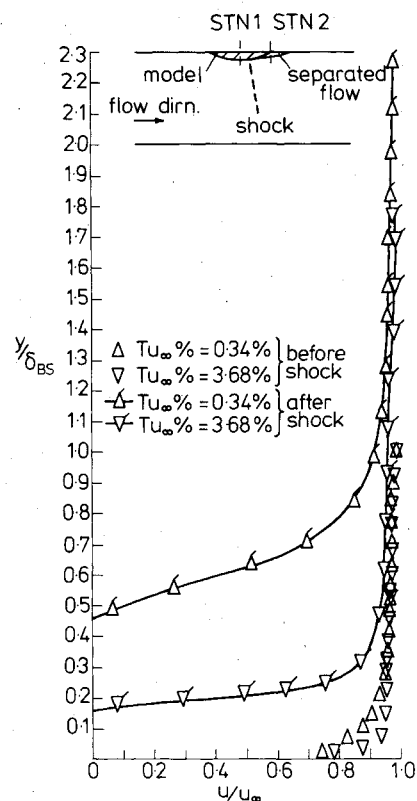


Fig. 1 Velocity profiles.

Received Oct. 15, 1982. Copyright © American Institute of Aeronautics and Astronautics, Inc., 1983. All rights reserved.

*Lecturer, Department of Aeronautical Engineering. Member AIAA.

†Research Student, Department of Aeronautical Engineering.